Velocity distribution function of a dilute gas under uniform shear flow: Comparison between a Monte Carlo simulation method and the Bhatnagar-Gross-Krook equation

J. Gómez Ordóñez, J. J. Brey, and A. Santos
Física Teórica, Universidad de Sevilla, Apartado 1065, 41080 Sevilla, Spain
(Received 17 July 1989)

A Monte Carlo simulation method is used to study a dilute gas of hard spheres under uniform shear flow in the hydrodynamic regime over a wide range of shear rates. The results for the components of the pressure tensor and also for the distribution function are presented and compared with those obtained by using the Bhatnagar-Gross-Krook model kinetic equation. The agreement is fairly good for the pressure tensor and also for the velocity distribution function in the small-velocity region, while discrepancies appear for large velocities. The possibility of using a maximum-entropy method to construct an approximate distribution function is discussed. It is shown that the inclusion of the pressure tensor leads to a distribution function significantly different from the one obtained in the simulation.

I. INTRODUCTION

Exact solutions to the Boltzmann equation are scarce. At the level of the velocity distribution function (VDF), the only solutions we are aware of refer either to spatially homogeneous systems[1] or to situations not directly related to transport problems.[2] There are two other solutions corresponding to more interesting physical situations, namely, uniform shear flow[2,3] and steady heat flow,[4] both for Maxwell molecules. In the first case, nonlinear expressions for the shear viscosity and the viscometric functions are obtained. In the second case, the heat flux is shown to be linear in the temperature gradient. Nevertheless, these two solutions are constructed by using the moment method, and explicit expressions for the distribution function are not known. In order to get information about the VDF in transport far from equilibrium, one can resort to computer simulations or tractable model kinetic equations.

Perhaps the most used model kinetic equation is the one proposed by Bhatnagar, Gross, and Krook[5] (BGK). The Boltzmann collision term is approximated by a relaxation term with a characteristic time that is modeled according to the interaction potential considered. The BGK equation keeps the main properties of the Boltzmann equation, namely the conservation of mass, momentum, and energy. An H theorem can also be proved for the BGK equation. However, little is known about the relationship between the solutions of the Boltzmann and the BGK equations for a given physical situation beyond the limit of small gradients.

In 1979, Zwanzig[6] derived an exact solution of the BGK model kinetic equation describing a system under uniform shear flow with arbitrary shear rate. For Maxwell molecules, the shear viscosity and the viscometric functions have explicit analytical expressions which coincide with those obtained from the Boltzmann equation.[2,3] In the case of hard spheres, Zwanzig was able to obtain a closed differential equation for the nonlinear shear viscosity. The hydrodynamic solution to this equation as a function of the shear rate has been numerically constructed.[7] Zwanzig also gave[6] a formal expression for the VDF, although its explicit form for the hydrodynamic regime was not discussed. On the other hand, in the context of the Boltzmann equation for hard spheres, only the first few terms of the Chapman-Enskog expansion are known.[8]

In this paper, we study a dilute gas of hard spheres under uniform shear flow by means of a Monte Carlo method to simulate the nonlinear Boltzmann equation.[9] This method allows one to follow the time evolution of the VDF, starting from arbitrary initial conditions. Of course, the moments can be easily obtained from the knowledge of the VDF. In particular, some results for the nonlinear shear viscosity were presented in a previous paper.[10] We were able to show that, after a transient period, the system reaches a hydrodynamic stage, independent of the initial conditions. Also, the simulation data were compared with the BGK results and an excellent agreement was found. Here, we extend the comparison to a wider range of shear rates and also to other components of the pressure tensor. Again, the agreement turns out to be quite good. Therefore, the BGK seems to be a fair approximation to the Boltzmann equation for the calculation of the first few moments. Regarding the VDF, we will see that the agreement is only qualitative. This is not surprising, since the detailed Boltzmann collision operator is replaced by a much simpler effective term in the BGK equation.

As said above, most of the solutions to the Boltzmann equation provide explicit expressions, exact or approximate, only for the first moments. A very interesting question is whether an accurate VDF can be constructed from the knowledge of those moments, as is the case in equilibrium situations. A standard method is to use information theory. As a test of its usefulness in far from equilibrium situations, we have used the pressure tensor obtained from the simulation to generate a maximum-

entropy VDF and compared it with the one provided by the simulation. The results show that the maximum-entropy criterion is not a very good one. This suggests the need for the search of alternative methods.

II. THE SIMULATION

The uniform shear flow (USF) state is characterized by a constant density, a spatially uniform temperature, and a local velocity field given by

$$u_i = a_{ij} r_j, \quad a_{ij} = a\,\delta_{ix}\delta_{jy} , \tag{2.1}$$

where a is the constant shear rate. Due to viscous heating effects, the temperature monotonically increases in time. It has been shown[11] that the Boltzmann equation admits a solution describing such a state when Lees-Edwards boundary conditions[12] are introduced. These are equivalent to periodic boundary conditions in the local rest frame.

For dilute gases, there exists a natural time scale defined from an effective collision frequency ν as

$$s(t) = \int_0^t dt' \nu(t') . \tag{2.2}$$

Thus, $s(t)$ is a measure of the number of collisions per particle between 0 and t. An expression for ν can be obtained from the Navier-Stokes shear viscosity $\eta_{\rm NS}$ (Ref. 5)

$$\nu = \frac{n k_B T}{\eta_{\rm NS}} , \tag{2.3}$$

where n is the number density, k_B is the Boltzmann constant, and T is the temperature. For hard spheres of diameter σ and mass m, one gets

$$\nu = \frac{8}{5}\left[\frac{2k_B T}{m\pi}\right]^{1/2} \lambda , \tag{2.4}$$

with λ being the mean free path,

$$\lambda = \frac{1}{\sqrt{2}\pi n \sigma^2} . \tag{2.5}$$

Therefore, ν is an increasing function of time due to viscous heating.

We have used the Boltzmann Monte Carlo method to simulate a system of hard spheres in the USF state. As discussed at length by Bird,[9] this method has been devised in order to mimic the dynamics described by the Boltzmann equation. Since the details of the method can be found in Ref. 9, we only give here the key points. At each time, both the position and velocity components of all the particles are stored. Their values are modified as the particles are followed through representative collisions and boundary interactions. The spatial volume is split into cells across which the change in flow properties is small. The molecular motion and the collisions are uncoupled over a time Δt small compared with the mean free time. In the collision process, the relative positions of the particles in each cell are disregarded and any pair of particles chosen at random forms a possible pair. The pair is accepted or rejected according to a probability that depends on the relative velocity and the interaction law. If accepted for collision, the post-collision velocity components are calculated from an appropriate random impact parameter and the pre-collision components. For each cell, a time counter is conveniently advanced after each collision. The collision process is repeated until the time counter exceeds the time step Δt.

Our system consists of N particles enclosed between two plates perpendicular to the y axis and separated by a distance L. In the simulation, the system is split into k layers parallel to the plates. These choices are based on the fact that in the USF only gradients along the y direction are present. In fact, just the y coordinate of the position of each particle, in addition to the three components of the velocity, are followed and recorded. To create a USF with shear rate a, a particle is reentered through the lower (upper) plate after it leaves the system through the upper (lower) one. In addition, the x component of the velocity is decreased (increased) by an amount equal to aL. As discussed above, the relevant time scale for the USF is the one defined by Eq. (2.2). Therefore, instead of considering a constant time step Δt, we have worked with a constant Δs, which for hard spheres corresponds to a $\Delta t \propto [T(t)]^{1/2}$.

From the simulation data, we compute the following quantities. The number of particles in layer α, N_α, is given by

$$N_\alpha = \sum_{l=1}^{N} \Theta_\alpha(y_l), \quad \alpha = 1, \ldots, k . \tag{2.6}$$

Here $\Theta_\alpha(y)$ is the characteristic function of layer α, i.e., $\Theta_\alpha(y)=1$ if y is inside the layer α, and $\Theta_\alpha(y)=0$ otherwise. The average velocity $\mathbf{u}_\alpha$, the temperature T_α, and the pressure tensor $P_{\alpha,ij}$ are

$$\mathbf{u}_\alpha = \frac{1}{N_\alpha}\sum_{l=1}^{N} \mathbf{v}_l \Theta_\alpha(y_l) , \tag{2.7}$$

$$\tfrac{3}{2} N_\alpha k_B T_\alpha = \tfrac{1}{2} m \sum_{l=1}^{N} (\mathbf{v}_l - \mathbf{u}_\alpha)^2 \Theta_\alpha(y_l) , \tag{2.8}$$

$$P_{\alpha,ij} = m \sum_{l=1}^{N} (v_{l,i} - u_{\alpha,i})(v_{l,j} - u_{\alpha,j})\Theta_\alpha(y_l) , \tag{2.9}$$

where $v_{l,i}$ is the i component of the velocity of particle l.

The knowledge of the velocity of all the particles allows one, in principle, to construct the VDF corresponding to layer α, $f_\alpha(\mathbf{v})$. However, this is an involved function to deal with, since it depends on the three velocity components. Consequently, we will focus on some reduced distributions that retain the main physical features, such as the distortions resulting from the fact that the system is far from equilibrium. Namely, we have considered

$$\Phi^{\pm}_{\alpha,x}(V_x) = \int_{-\infty}^{\infty} dv_y \int_{-\infty}^{\infty} dv_z H(\pm v_y \mp u_{\alpha,y}) f_\alpha(\mathbf{v}) , \quad V_x \equiv v_x - u_{\alpha,x} , \tag{2.10a}$$

$$\Phi^{\pm}_{\alpha,x}(V_y) = \int_{-\infty}^{\infty} dv_x \int_{-\infty}^{\infty} dv_z H(\pm v_x \mp u_{\alpha,x}) f_\alpha(\mathbf{v}) , \quad V_y \equiv v_y - u_{\alpha,y} , \tag{2.10b}$$

where $H(x)$ is Heaviside's step function. To obtain the VDF from the simulation data, one has to consider finite velocity intervals. Thus, what is actually computed are the discretized versions of Eqs. (2.10). For instance,

$$\Phi^{\pm}_{\alpha,y}(V_y)=\frac{1}{\Delta V_y}\sum_{l=1}^{N} H(v_{l,y}-u_{\alpha,y}-V_y+\tfrac{1}{2}\Delta V_y) \times H(V_y+\tfrac{1}{2}\Delta V_y-v_{l,y}+u_{\alpha,y}) \times H(\pm v_{l,x}\mp u_{\alpha,x})\Theta_{\alpha}(y_l) . \quad (2.11)$$

Therefore, $\Phi^{+}_{\alpha,y}(V_y)\Delta V_y$ represents the number of particles in layer α having a velocity $\mathbf{v}$ with components such that

$$v_x-u_{\alpha,x}>0, \quad V_y-\tfrac{1}{2}\Delta V_y<v_y-u_{\alpha,y}<V_y+\tfrac{1}{2}\Delta V_y ,$$

and arbitrary v_z. Analogously, one can define $\Phi^{+}_{\alpha,x}(V_x)\Delta V_x$ for particles with $v_y-u_{\alpha,y}>0$ and

$$V_x-\tfrac{1}{2}\Delta V_x<v_x-u_{\alpha,x}<V_x+\tfrac{1}{2}\Delta V_x .$$

All the above quantities are in general functions of time and position, the latter being measured by the index α. Nevertheless, in the USF state only $u_{\alpha,x}$ depends on α, all the other quantities being uniform across the system. We have checked that our simulation maintains in time the features of the USF state when starting from appropriate initial conditions. Therefore, in order to improve the statistics, we have averaged over the layers to obtain the temperature T and the pressure tensor P_{ij}. For the VDF, in addition to the homogeneity, the symmetry of the state requires that

$$\Phi^{+}_{x}(V_x)=\Phi^{-}_{x}(-V_x), \quad \Phi^{+}_{y}(V_y)=\Phi^{-}_{y}(-V_y) .$$

Thus, what we have actually computed from the simulation is

$$\tfrac{1}{2}[\Phi^{+}_{x}(V_x)+\Phi^{-}_{x}(-V_x)] ,$$

although we keep the notation $\Phi^{+}_{x}(V_x)$ because of the above symmetry property. We have proceeded in a similar way for $\Phi^{+}_{y}(V_y)$.

We have considered the following values of the simulation parameters: $N=2000$ particles, $L=10\lambda$, $k=40$ layers, and $\Delta s=0.016/\sqrt{\pi}$. Also, the results we will report correspond to averages over $\mathcal{N}=200$ different realizations. The statistical error of a given quantity $A(t)$ has been estimated by first evaluating the standard deviation $\Delta_{\mathcal{N}_1}A(t)$ of the averages corresponding to 10 blocks of $\mathcal{N}_1=20$ realizations each. Then, assuming that the error decreases as $\mathcal{N}^{-1/2}$, we get

$$\Delta_{\mathcal{N}}A(t)=(\mathcal{N}_1/\mathcal{N})^{1/2}\Delta_{\mathcal{N}_1}A(t) .$$

III. RESULTS

We are interested in the hydrodynamic regime, where the evolution of the system does not depend on the initial condition. In a previous paper[10] we have shown that such a regime can be identified by comparing the evolution corresponding to different initial conditions.

In the USF, the hydrodynamic dimensionless VDF must be a function of $\mathbf{V}^*\equiv(\mathbf{v}-\mathbf{u})/\sqrt{2k_BT/m}$ and $a^*\equiv a/\nu$, where ν is given by Eq. (2.3) and, therefore, depends on time through the temperature. In fact, a^* is the uniformity parameter of the system, measuring the ratio between the mean free path and the characteristic hydrodynamic length. Consistently, the hydrodynamic dimensionless pressure tensor is just a function of a^*. It must be noticed that a^* decreases in time, so that the system asymptotically tends towards local equilibrium.

First, we discuss the results obtained for the pressure tensor. Figure 1 shows the behavior of the generalized shear viscosity, defined as

$$\eta^*(a^*)=-\frac{P^*_{xy}}{a^*} , \quad (3.1)$$

where $P^*_{ij}=P_{ij}/p$, p being the hydrostatic pressure. The simulation data are compared with the shear viscosity obtained from the BGK equation for hard spheres[7] and from the Boltzmann equation for Maxwell molecules.[2,3] The simulation was started with an initial condition corresponding to $a^{*2}=10^4$. Therefore, the reported values of η^* can be considered as hydrodynamic.[10] Quite good agreement is found in both cases. In particular, the BGK equation turns out to be a very good approximation to the Boltzmann equation for the calculation of the shear viscosity in this system. It must be noticed that the agreement appears over a very wide range of values of a^*. In fact, the behavior of the simulation data for large a^* is consistent with an asymptotic decay of the form $\eta^*\sim a^{*-4/3}$, as predicted by the Boltzmann equation for Maxwell molecules and also by the BGK equation for any potential. This extends the conclusion reached in Ref. 10, where only the region $0<a^*<1$ was considered.

To analyze the behavior of the diagonal elements of the pressure tensor, we introduce the viscometric functions

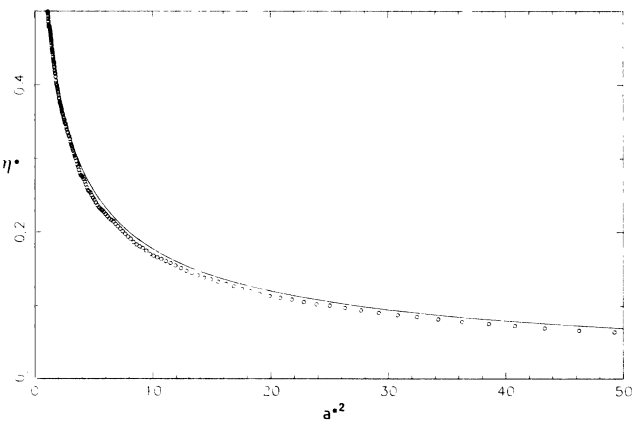

FIG. 1. Reduced shear viscosity $\eta^*(a^*)$. The circles are simulation data, the solid line corresponds to the BGK equation for hard spheres, and the dotted line corresponds to the Boltzmann equation for Maxwell molecules. The error bars in the simulation lie inside the circles.

$$\Psi_1(a^*)=(P^*_{yy}-P^*_{xx})/a^{*2}\ , \tag{3.2}$$

$$\Psi_2(a^*)=(P^*_{zz}-P^*_{yy})/a^{*2}\ . \tag{3.3}$$

It is seen in Fig. 2 that the BGK equation reproduces the simulation data for $\Psi_1(a^*)$ very well. Although the same qualitative behavior is also obtained from the Boltzmann equation for Maxwell molecules, the quantitative agreement is not so good. We have observed the same tendency for values of a^* much larger than the ones reported here. On the other hand, very small values of a^* are hard to obtain in computer simulations, since they require a huge number of collisions and, therefore, a lot of computer time. Nevertheless, there is no reason to expect a worse agreement for $a^{*2}\leq 0.2$. In particular, the Chapman-Enskog expansion up to the Burnett order leads to $\Psi_1=-2.028$ for hard spheres.[8]

Both the BGK equation and the Boltzmann equation for Maxwell molecules yield $\Psi_2(a^*)=0$, while the Chapman-Enskog expansion for hard spheres gives $\Psi_2=0.172$ in the limit $a^*\to 0$.[8] The results of the simulation, shown in Fig. 3, give a Ψ_2 definitely different from zero, and also a tendency for $a^*\to 0$ that is consistent with the Chapman-Enskog value. Therefore, both the kinetic equation and the interaction potential play an important role in the determination of the viscometric function $\Psi_2(a^*)$. Nevertheless, given the small value of Ψ_2, one can conclude in summary that the BGK equation gives a fair approximation to the pressure tensor for a dilute gas under USF.

Let us now check whether the above conclusion also applies to the VDF. We have considered the dimensionless distributions

$$R^+_x(V^*_x,a^*)=\frac{\Phi^+_x(V_x,t)}{F^+_x(V_x,t)}\ , \tag{3.4}$$

$$R^+_y(V^*_y,a^*)=\frac{\Phi^+_y(V_y,t)}{F^+_y(V_y,t)}\ , \tag{3.5}$$

where Φ^+_x and Φ^+_y have been defined in Sec. II, and F^+_x and F^+_y are the corresponding local equilibrium expressions, namely,

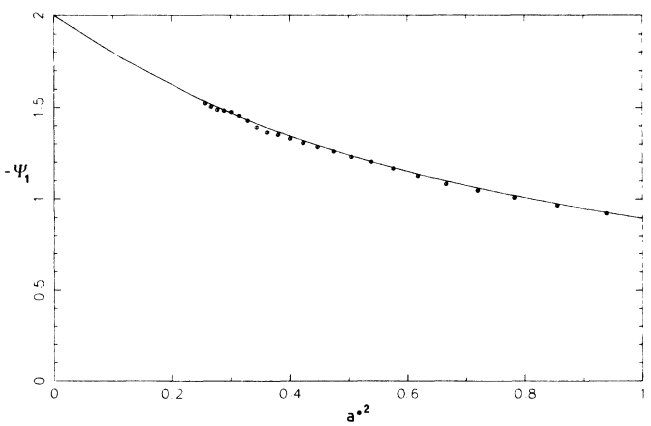

FIG. 2. The same as Fig. 1 but for the first viscometric function $\Psi_1(a^*)$.

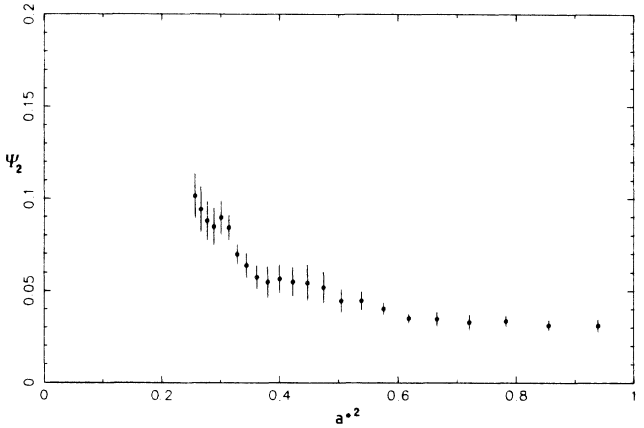

FIG. 3. Simulation data for the second viscometric function $\Psi_2(a^*)$. Notice the change of scale as compared to Fig. 2.

$$F^+_x(V_x,t)=\frac{1}{2}\frac{N}{k}\left[\frac{m}{2\pi k_B T(t)}\right]^{1/2} e^{-mV_x^2/2k_BT(t)}\ , \tag{3.6}$$

and equivalently for F^+_y.

In Figs. 4 and 5, we compare R^+_x and R^+_y, respectively, for $a^{*2}=0.85$, as obtained from the simulation data and from the BGK equation.[13] It is clear that there are significant discrepancies, especially in the high-velocity region, although the qualitative behavior in the small velocity region is quite similar. In particular, we notice that the BGK equation predicts fairly well the position and symmetry of the maximum in Fig. 5. The disagreement for high velocities is not surprising, since the evolution of the VDF in the BGK equation is governed by only the first five moments.

A very interesting problem in nonequilibrium statistical mechanics is the construction of the distribution function of the system starting from the knowledge of the transport properties. If one uses information theory, it is

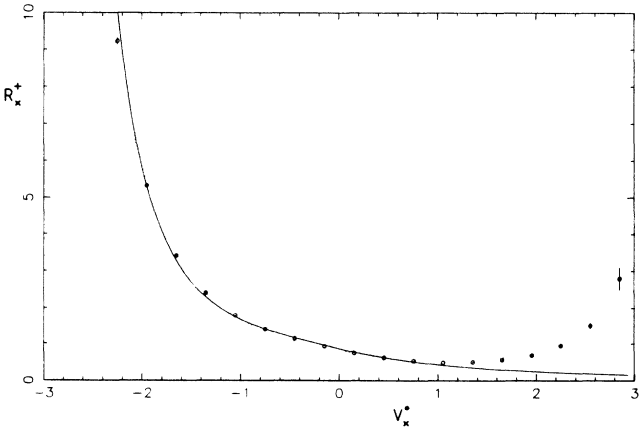

FIG. 4. Relative distribution function $R^+_x(V^*_x)$, defined by Eq. (3.4), for $a^{*2}=0.85$. The circles are simulation data, the solid line corresponds to the BGK equation for hard spheres, and the dotted line corresponds to the maximum-entropy function.

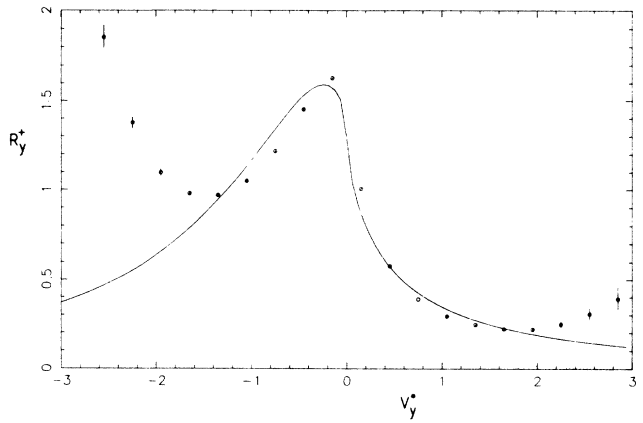

FIG. 5. The same as Fig. 4 but for the function $R_y^+(V_y^*)$, defined by Eq. (3.5).

clear that the knowledge of the hydrodynamic fields is not enough, since it leads to a local equilibrium distribution. Here, we have explored the possibility of building an approximate VDF for a dilute gas under USF by assuming that the pressure tensor is given. Therefore, we look for a VDF $\tilde{f}(\mathbf{V})$ maximizing the entropy

$$S=-\int d\mathbf{V}\,\tilde{f}\ln\tilde{f} \tag{3.7}$$

under the constraints

$$\int d\mathbf{V}\,\tilde{f}=n\ , \tag{3.8}$$

$$\int d\mathbf{V}\,\mathbf{V}\tilde{f}=0\ , \tag{3.9}$$

and

$$\int d\mathbf{V}\,V_iV_j\tilde{f}=\frac{1}{m}P_{ij}\ . \tag{3.10}$$

Then, $\tilde{f}$ has the form

$$\tilde{f}(\mathbf{V})=n\pi^{-3/2}(\det A)^{1/2}e^{-A_{ij}V_iV_j}\ , \tag{3.11}$$

where

$$A_{ij}=\tfrac{1}{2}mn(P^{-1})_{ij}\ . \tag{3.12}$$

Using the pressure tensor from the simulation, we have also plotted in Figs. 4 and 5 the functions R_x^+ and R_y^+ corresponding to the maximum-entropy distribution (3.11). As was the case for the BGK equation, the agreement is better for R_x^+ than for R_y^+. In any case, $\tilde{f}$ is not able to reproduce the details of the actual VDF of the system. For instance, $\tilde{f}$ leads to a shifted maximum in Fig. 5, R_y^+ being quite symmetrical around it. In fact, Figs. 4 and 5 show three distributions giving the same values for the hydrodynamic fields and very close values for the pressure tensor, but having quite different shapes.

IV. CONCLUSIONS

In this paper we have used a Monte Carlo simulation method to study a dilute gas of hard spheres under uniform shear flow. The components of the pressure tensor have been obtained over a wide range of shear rate values and compared, first, with those obtained from the Boltzmann equation for Maxwell molecules and, second, with those from the BGK model kinetic equation for hard spheres.

The first comparison shows a fairly good agreement, indicating that the influence of the interaction potential on the transport properties is not very strong when quantities are properly scaled. In this context, it is worth mentioning that very recently Loose[14] has compared molecular-dynamics results for a dilute Lennard-Jones gas under USF with an approximate solution to the Boltzmann equation. This solution turns out to be the exact one for Maxwell molecules. He also found a good agreement, which confirms the weak influence of the interaction potential.

On the other hand, the agreement is much better when the comparison is carried out with the BGK model for hard spheres. This indicates that the nonlinear BGK equation provides a very useful tool to get approximate transport properties in far from equilibrium situations. In fact, as mentioned in the Introduction, the pressure tensor under USF obtained from the Boltzmann equation and from the BGK equation coincides for Maxwell molecules for all values of the reduced shear rate.

A much more difficult problem is to obtain the nonequilibrium VDF of the system. In particular, no exact solution to the Boltzmann equation at this level is known for the USF, even in the case of Maxwell molecules. The comparison between the simulation and the BGK model shows a good agreement for small velocities but significant discrepancies appear in the high-velocity region. This leads us to conclude that the BGK equation is a good approximation for low moments of the distribution but fails for high moments. This is consistent with the results obtained by Loose and Hess[15] by using a moment-expansion method for the Boltzmann equation.

We have also explored the applicability of the information theory method to determine the VDF of a system in a far from equilibrium situation. The results show that the knowledge of the fluxes, the pressure tensor in our case, is not enough to get an accurate distribution. Besides, the addition of the next order moments is not expected to produce a significant improvement. This fact emphasizes the importance of nonlocal effects in far from equilibrium situations. While the distribution function based on information theory is always a local functional of a finite number of moments, the solution of the BGK equation is a nonlocal functional of the first five moments. This nonlocal character makes the BGK equation to be a much better approximation to the Boltzmann equation. In addition, the information theory method requires the knowledge of the first moments, while they are self-consistently obtained in the BGK equation.

ACKNOWLEDGMENTS

We acknowledge partial support from the Dirección General de Investigación Científica y Técnica (Spain) through Grant No. PB 86-0205.

[1]M. H. Ernst, Phys. Rep. **78**, 1 (1981).
[2]For a review and extensive bibliography, see C. Truesdell and R. G. Muncaster, *Fundamentals of Maxwell's Kinetic Theory of a Simple Monatomic Gas* (Academic, New York, 1980).
[3]E. Ikenberry and C. Truesdell, J. Ration. Anal. **5**, 1 (1956); **5**, 128 (1956).
[4]E. S. Asmolov, N. K. Makarhev, and V. I. Nosik, Dokl. Akad. Nauk. SSSR **249**, 577 (1979) [Sov. Phys.—Dokl. **24**, 892 (1979)].
[5]C. Cercignani, *The Boltzmann Equation and Its Applications* (Springer-Verlag, New York, 1988).
[6]R. Zwanzig, J. Chem. Phys. **71**, 4416 (1979).
[7]A. Santos, J. J. Brey, and J. W. Dufty, Phys. Rev. Lett. **56**, 1571 (1986).
[8]S. Chapman and T. G. Cowling, *The Mathematical Theory of Non-Uniform Gases* (Cambridge University Press, Cambridge, 1970).
[9]G. Bird, *Molecular Gas Dynamics* (Clarendon, Oxford, 1976); Phys. Fluids **13**, 2676 (1970).
[10]J. Gómez Ordóñez, J. J. Brey, and A. Santos, Phys. Rev. A **39**, 3038 (1989).
[11]J. W. Dufty, A. Santos, J. J. Brey, and R. F. Rodríguez, Phys. Rev. A **33**, 459 (1986).
[12]A. Lees and S. Edwards, J. Phys. C **5**, 1921 (1972).
[13]A. Santos, J. J. Brey, and J. Gómez Ordóñez (unpublished).
[14]W. Loose, Phys. Lett. A **128**, 39 (1988).
[15]W. Loose and S. Hess, Phys. Rev. A **37**, 2099 (1988).